# Investigation of Sequence Parameters of Overhead Transmission Lines Located on Soils with Frequency-Dependent Electrical Parameters

Tainá Fernanda Garbelim Pascoalato
*Department of Electrical Engineering*
*São Paulo State University (UNESP)*
Ilha Solteira, Brazil
tfg.pascoalato@unesp.br

Anderson Ricardo Justo de Araújo
*School of Engineering*
*Cardiff University*
Cardiff, UK
justodearaujoa@cardiff.ac.uk

Sérgio Kurokawa
*Department of Electrical Engineering*
*São Paulo State University (UNESP)*
Ilha Solteira, Brazil
sergio.kurokawa@unesp.br

José Pissolato Filho
*School of Electrical and Computer Eng.*
*University of Campinas (UNICAMP)*
Campinas, Brazil
pisso@unicamp.br

***Abstract*—This paper examines the effects of ground-return parameters (impedance and admittance) and frequency-dependent soil electrical parameters on the sequence parameters of symmetrical circuits (zero, positive, and negative) in a double-circuit transmission line, using Nakagawa's approach. An analysis was conducted on three distinct transmission towers (Danube, Flat, and Ton) situated on soil with a low-frequency resistivity of 1,000 Ω.m over a frequency range from 100 Hz to 1 MHz. The results indicate that zero-sequence resistance and inductance are significantly greater than those of the positive sequence. Conversely, positive-sequence capacitance exceeds zero-sequence capacitance, which varies at high frequencies due to ground-return admittance. Additionally, coupling factors for individual circuits and between both circuits were evaluated, revealing that the coupling factor within one circuit can generally be ignored. However, the coupling factor for zero-sequence admittance is substantial, influenced by tower topology and frequency range. The numerical results highlight the strong magnetic and electric coupling between circuits in the zero sequence for untransposed double-circuit overhead transmission lines.**

***Index Terms*—transmission lines, sequence parameters, ground-return effects, soil modeling, symmetric components**

## I. Introduction

Adequate computation of the symmetrical components, and its sequence parameters, of a transmission line (TL) is essential for the effective design, operation, and maintenance of power systems. In this context, the sequence parameters are import to accurately determine the fault detection and protection in transmission lines [1]–[5], power flow analysis and line parameter estimation [6], [7] and harmonics in power quality studies [8].

This work was supported by the Coordenação de Aperfeiçoamento de Pessoal de Nível Superior (CAPES) - Finance code 001 and by São Paulo Research Foundation (FAPESP) (grant: 2019/01396-1, 2020/10141-4 and 2022/09182-3).

To compute the sequence (zero, positive and negative) parameters of the transmission line, firstly, the longitudinal impedance $\boldsymbol{Z}_\ell$ and transversal admittance $\boldsymbol{Y}_{\mathrm{t}}$ matrices must be correctly assessed considering the soil on which the TL is located and the tower geometry.

Regarding the consideration of the soil, this is done through the ground-return impedance ($Z_{\mathrm{g}}$), the ground-return admittance ($Y_{\mathrm{g}}$) and the soil's electrical parameters ($\rho_{\mathrm{g}}$ and $\varepsilon_{\mathrm{r}}$). There are several methods used in the literature to determine the ground-return parameters ($Z_{\mathrm{g}}$ and $Y_{\mathrm{g}}$), such as Carson and Nakagawa [9], [10]. The Carson model is considered a more conservative approach, as it neglects the displacement currents in the soil and assumes a constant soil resistivity. In contrast, the Nakagawa model is seen as a more realistic approach, as it allows the soil's electrical parameters to vary with frequency and takes into account the displacement currents in the soil.

Concerning the tower geometry, the ground wires effect must be reduced in the $\boldsymbol{Z}_\ell$ and $\boldsymbol{Y}_{\mathrm{t}}$ matrices using the Kron's reduction technique. Subsequently, the sequence impedance matrices $\boldsymbol{Z}_{\mathrm{sym}}$ and $\boldsymbol{Y}_{\mathrm{sym}}$ are calculated using the longitudinal impedance $\boldsymbol{Z}_\ell$ and transversal admittance $\boldsymbol{Y}_{\mathrm{t}}$ matrices using a transformation matrix, denoted here as $\mathbf{S}$, which is dependent on the complex number $\alpha = e^{j120^\circ}$.

When the $n$-phase transmission line has a complete transposition configuration, the resulting matrices $\boldsymbol{Z}_\ell$ and $\boldsymbol{Y}_{\mathrm{t}}$ are symmetrical, having identical mutual elements on the off-diagonal, i.e. $X_{12} = X_{13}$; and identical diagonal elements, i.e. $X_{11} = X_{22} = ...X_{\mathrm{nn}}$ . This symmetry facilitates the computation of the sequence impedance matrices $\boldsymbol{Z}_{\mathrm{sym}}$ and $\boldsymbol{Y}_{\mathrm{sym}}$, where the sequence parameters are readily obtained from the main diagonal elements and the remaining elements are zero [11], [12]. On the other hand, when the $n$-phase transmission line has a untransposed configuration, the matrices $\boldsymbol{Z}_\ell$ and

$\boldsymbol{Y}_{\mathrm{t}}$ might have different self- and off-diagonal elements, due to the distinct heights and distances between the conductors, representing the mutual coupling. Consequently, the sequence impedance and admittance matrices have non zero off-diagonal elements, meaning that symmetrical sequence is neither magnetically nor electrically decoupled in their sequence circuits [11], [12].

In [8], the authors investigated the sequence parameters (resistance, inductance, and capacitance) and coupling effects using symmetrical components for three distinct 110-kV transmission tower topologies (Danube, Flat, and Ton), employing Carson's approach, frequency-constant soil parameters, and a limited frequency range from 50 Hz to 20 kHz. The results demonstrated a significant dependence of the sequence parameters on the frequency range and highlighted the necessity of considering strong coupling between circuits. To the best of the author's knowledge, there has been no investigation in the literature that examines the sequence parameters of double-circuit transmission lines, considering ground-return parameters (impedance and admittance) using Nakagawa's approach and frequency-dependent soil properties.

This paper investigates the impact of the ground-return effect and frequency-dependent soil electrical parameters using Nakagawa's approach on the sequence parameters (resistance, inductance, and capacitance) in the symmetrical circuits (zero, positive, and negative) of a double-circuit transmission line. Three distinct towers (Danube, Flat, and Ton) located on soil with a low-frequency resistivity of $1,000$ $\Omega$.m were analyzed for a frequency range from 100 Hz to 1 MHz. The results demonstrated that the zero-sequence resistance and inductance are significantly higher than the positive sequence. However, the positive capacitance is higher than the zero-sequence capacitance, which varies at high frequencies due to the ground-return admittance. Additionally, the coupling factors for individual circuits and between both circuits are calculated for the double-circuit transmission lines. Results demonstrated that the coupling factor within one circuit can be neglected. However, the coupling factor for the zero-sequence admittance can be considerable depending on the tower topology and across the frequency range. These results confirm that the magnetic and electric coupling between both circuits in the zero sequence is very strong for untransposed double-circuit overhead transmission lines.

As a contribution, this work has shown that untransposed double-circuit transmission lines exhibit strong coupling between the sequence circuits. These couplings cannot be neglected for untransposed transmission lines, especially if high-frequency events are involved in the simulations.

## II. Power system modeling

### A. Transmission line

The Telegrapher's equations are a pair of differential equations that describe voltages ($\boldsymbol{V}(\omega)$) and currents ($\boldsymbol{I}(\omega)$) along the length of a multi-conductor overhead transmission line as follows [13]

$$\frac{\partial \boldsymbol{V}(\omega)}{\partial x} = -\boldsymbol{Z}_{\ell}(\omega)\boldsymbol{I}(\omega), \tag{1}$$

$$\frac{\partial \boldsymbol{I}(\omega)}{\partial x} = -\boldsymbol{Y}_{\mathrm{t}}(\omega)\boldsymbol{V}(\omega), \tag{2}$$

where the longitudinal impedance $\boldsymbol{Z}_{\ell}(\omega)$ [$\Omega$/m] and transversal admittance $\boldsymbol{Y}_{\mathrm{t}}(\omega)$ [S/m] matrices are expressed by

$$\boldsymbol{Z}_{\ell}(\omega) = \boldsymbol{Z}_{\mathrm{i}}(\omega) + \boldsymbol{Z}_{\mathrm{e}}(\omega) + \boldsymbol{Z}_{\mathrm{g}}(\omega), \tag{3}$$

$$\boldsymbol{Y}_{\mathrm{t}}(\omega) = \left[\boldsymbol{Y}_{\mathrm{e}}^{-1}(\omega) + \boldsymbol{Y}_{\mathrm{g}}^{-1}(\omega)\right]^{-1}, \tag{4}$$

where $\omega = 2\pi f$ is the angular frequency [rad/s], $f$ is the frequency [Hz], $\boldsymbol{Z}_{\mathrm{i}}(\omega)$ is the internal impedance [$\Omega$/m], $\boldsymbol{Z}_{\mathrm{e}}(\omega)$ is the external impedance [$\Omega$/m] and $\boldsymbol{Z}_{\mathrm{g}}(\omega)$ is the ground-return impedance [$\Omega$/m] associated to the penetrating magnetic field that generates induced currents into the soil. In (4), $\boldsymbol{Y}_{\mathrm{e}}(\omega)$ is the external admittance [S/m] considering a perfect soil and $\boldsymbol{Y}_{\mathrm{g}}(\omega)$ is the ground-return admittance [S/m] corresponding to a correction term for lossy soil with frequency-dependent electrical parameters that must be added.

*1) Ground-return parameters:* The ground-return impedance $\boldsymbol{Z}_{\mathrm{g}}(\omega)$ can be calculated by

$$Z_{\mathrm{g_{ii}}}(\omega) = j\frac{\omega\mu_0}{\pi}\int_0^{\infty}\frac{e^{-2h_{\mathrm{i}}\lambda}}{\sqrt{\lambda^2+\gamma_{\mathrm{g}}^2}+\lambda}d\lambda, \tag{5}$$

$$Z_{\mathrm{g_{ij}}}(\omega) = j\frac{\omega\mu_0}{\pi}\int_0^{\infty}\frac{e^{-(h_{\mathrm{i}}+h_{\mathrm{j}})\lambda}}{\sqrt{\lambda^2+\gamma_{\mathrm{g}}^2}+\lambda}\cos(r_{\mathrm{ij}}\lambda)d\lambda, \tag{6}$$

$$\gamma_{\mathrm{g}}^2 = j\omega\mu_0[\sigma_{\mathrm{g}} + j\omega(\varepsilon_{\mathrm{r}}-k)\varepsilon_0], \tag{7}$$

where $\mu_0$ is the vacuum magnetic permeability ($\mu_0 = 4\pi\times10^{-7}$ [H/m]), $\sigma_{\mathrm{g}}$ is the soil conductivity [S/m], $\varepsilon_{\mathrm{r}}$ is the relative permittivity and $\varepsilon_0$ is the vacuum permittivity ($\varepsilon_0 = 8.85\times10^{-12}$ [F/m]). Regarding the geometrical parameters, $h_{\mathrm{i}}$ and $h_{\mathrm{j}}$ are the heights of the conductors $i$ and $j$ in relation to the ground level [m], $r_{\mathrm{ij}}$ is the horizontal distance between the conductors $i$ and $j$ [m] and $\lambda$ is an integration variable. The $k$ is a correction factor. If $k = 1$ in (7), the equations (5) and (6) are represented by Nakagawa's approach [10]. Otherwise, if $k = \varepsilon_{\mathrm{r}}$, these equations are reduced to Carson's approach [9]. Regarding the ground-return admittance, Nakagawa proposed the following expression [10]

$$\boldsymbol{Y}_{\mathrm{g}}(\omega) = j\omega[\boldsymbol{P}_{\mathrm{g}}(\omega)]^{-1}, \tag{8}$$

$$P_{\mathrm{g_{ii}}}(\omega) = \frac{1}{\pi\varepsilon_0}\int_0^{\infty}\frac{e^{-2h_{\mathrm{i}}\lambda}}{\frac{\lambda\gamma_1^2}{\gamma_0^2}+\alpha_1}d\lambda, \tag{9}$$

$$P_{\mathrm{g_{ij}}}(\omega) = \frac{1}{\pi\varepsilon_0}\int_0^{\infty}\frac{e^{-(h_{\mathrm{i}}+h_{\mathrm{j}})\lambda}}{\frac{\lambda\gamma_1^2}{\gamma_0^2}+\alpha_1}\cos(r_{\mathrm{ij}}\lambda)d\lambda, \tag{10}$$

$$\alpha_1 = \sqrt{\lambda^2+\gamma_1^2-\gamma_0^2}, \tag{11}$$

$$\gamma_0^2 = -\omega^2\mu_0\varepsilon_0, \quad \gamma_1^2 = j\omega\mu_0(\sigma_{\mathrm{g}} + j\omega\varepsilon_{\mathrm{r}}\varepsilon_0). \tag{12}$$

*2) Electrical parameters of soil:* Soil can be represented by its electrical parameters *i.e.* magnetic permeability ($\mu_g$), resistivity ($\rho_g$), and relative permittivity ($\varepsilon_r$). It is known in the literature that the resistivity ($\rho_g$) and relative permittivity ($\varepsilon_r$) are significantly variable with the frequency. However, the magnetic permeability is assumed equal to the magnetic permeability of free space ($\mu_0$).

This phenomenon is related to the several polarization processes (molecular, ionic, and electronic) occurring in the soil particles as the frequency increases. Consequently, when the frequency dependency is considered on the soil parameters, the soil's conductivity increases and the relative permittivity decreases as the frequency increases. The frequency-dependent resistivity and permittivity are calculated as closed-form expressions, being these expressions recommended by CIGRÈ WG, give as follows [14]

$$\rho_g(f) = \rho_0 \left\{1 + 4.7 \times 10^{-6} f^{0.54} \rho_0^{0.73}\right\}^{-1}, \tag{13}$$

$$\varepsilon_r(f) = 12 + 9.5 \times 10^{4} \rho_0^{-0.27} f^{-0.46}, \tag{14}$$

where $\rho_0$ is the low-frequency resistivity measured at 100 Hz [Ω.m]. The soil resistivity and relative permittivity assuming a low frequency resistivity $\rho_0$ of 1,000 Ω.m is plotted in Fig. 1

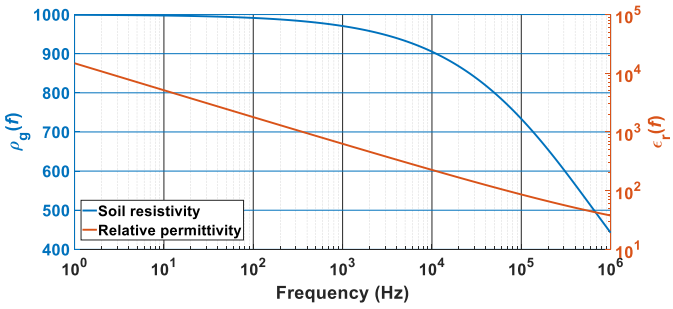


Fig. 1: Soil resistivity (in blue) and relative permittivity (in orange) for a low frequency resistivity $\rho_0$ as a function of frequency.

According to this figure, the soil resistivity $\rho_g$ is strongly dependent on the frequency, where the soil becomes more conductive as the frequency increases and the reduction in the soil resistivity is more noticeable at the high frequencies. Furthermore, the permittivity $\varepsilon_r$ decreases for the increasing frequency due to the several polarization mechanisms occurring in the soil particles [14].

*3) Kron's reduction:* The ground wires in a transmission line (TL) can be represented either implicitly or explicitly depending on the type of analysis [15]. When using the explicit representation, the ground wires are considered additional conductors of a given TL. However, in the implicit representation, the effects of the ground wires (either grounded or isolated) are reflected on the phase conductors. In this way, the TL is seen as having only ($n_p$) equivalent conductors. Consequently, the longitudinal impedance and transversal admittance matrices are reduced (order $n_p \times n_p$), which reduces the computational time for calculating electromagnetic transients in power systems [15]. In this work, the implicit representation of the ground wires will be used. Considering that (3) and (4) represent a multi-phase transmission line with $n$ phases (where $n = n_p + n_w$), the longitudinal impedance matrix $\boldsymbol{Z}_\ell(\omega)$ and the transversal admittance matrix $\boldsymbol{Y}_t(\omega)$, both with $n \times n$, can be organized into matrices expressed in the form [16]

$$\begin{bmatrix} \boldsymbol{V}_{pp} \\ \boldsymbol{V}_{ww} \end{bmatrix} = \begin{bmatrix} \boldsymbol{Z}_{pp} & \boldsymbol{Z}_{pw} \\ \boldsymbol{Z}_{wp} & \boldsymbol{Z}_{ww} \end{bmatrix} \begin{bmatrix} \boldsymbol{I}_{pp} \\ \boldsymbol{I}_{ww} \end{bmatrix}, \tag{15}$$

$$\begin{bmatrix} \boldsymbol{V}_{pp} \\ \boldsymbol{V}_{ww} \end{bmatrix} = \begin{bmatrix} \boldsymbol{P}_{pp} & \boldsymbol{P}_{pw} \\ \boldsymbol{P}_{wp} & \boldsymbol{P}_{ww} \end{bmatrix} \begin{bmatrix} \boldsymbol{Q}_{pp} \\ \boldsymbol{Q}_{ww} \end{bmatrix}, \tag{16}$$

where $\boldsymbol{Q}$ are the charges accumulated on the TL [C] and $\boldsymbol{P}$ is the matrix of Maxwell's potential coefficients [km/F]. The subscripts pp and ww are related to the phase conductors and ground wires, respectively. The subscripts pw and wp represent mutual elements between the phase conductors and ground wires. In this case, the sub-matrices corresponding to the subscripts pw and wp have the property of being transposes of each other. The impedance and admittance matrices are

$$\boldsymbol{Z}_\ell = \begin{bmatrix} \boldsymbol{Z}_{pp} & \boldsymbol{Z}_{pw} \\ \boldsymbol{Z}_{wp} & \boldsymbol{Z}_{ww} \end{bmatrix} = \begin{bmatrix} \boldsymbol{R}_{pp} + j\omega\boldsymbol{L}_{pp} & \boldsymbol{R}_{pw} + j\omega\boldsymbol{L}_{pw} \\ \boldsymbol{R}_{wp} + j\omega\boldsymbol{L}_{wp} & \boldsymbol{R}_{ww} + j\omega\boldsymbol{L}_{ww} \end{bmatrix}, \tag{17}$$

$$\boldsymbol{Y}_t = \begin{bmatrix} \boldsymbol{Y}_{pp} & \boldsymbol{Y}_{pw} \\ \boldsymbol{Y}_{wp} & \boldsymbol{Y}_{ww} \end{bmatrix} = j\omega \begin{bmatrix} \boldsymbol{C}_{pp} & \boldsymbol{C}_{pw} \\ \boldsymbol{C}_{wp} & \boldsymbol{C}_{ww} \end{bmatrix} = j\omega \begin{bmatrix} \boldsymbol{P}_{pp} & \boldsymbol{P}_{pw} \\ \boldsymbol{P}_{wp} & \boldsymbol{P}_{ww} \end{bmatrix}^{-1}, \tag{18}$$

where the sub-matrix $\boldsymbol{Z}_{pp}$ ($n_p \times n_p$) represents the self and mutual elements for the phase conductors only, the sub-matrices $\boldsymbol{Z}_{pw}$ ($n_p \times n_w$) and $\boldsymbol{Z}_{wp}$ ($n_w \times n_p$) represent the mutual elements between the phase conductors and the ground wires, and the sub-matrix $\boldsymbol{Z}_{ww}$ ($n_w \times n_w$) represents the self and mutual elements for the ground wires. Similarly, the same subscripts apply to the sub-matrices $\boldsymbol{Y}_{pp}$, $\boldsymbol{Y}_{pw}$, $\boldsymbol{Y}_{wp}$, and $\boldsymbol{Y}_{ww}$. The element $\boldsymbol{R}$ is the resistance matrix [Ω/m], $\boldsymbol{L}$ is the inductance matrix [H/m] (both considering the skin effect), and $\boldsymbol{C}$ is the capacitance matrix [F/m] [17]. When the ground wires are continuously grounded at each tower structure, and the tower impedance can be neglected, the voltage drop between two terminals of a ground wire is approximately zero [16]. In this case, the voltage drop in the ground wires $[\boldsymbol{V}_{ww}] \approx 0$, and thus (17) and (18) can be rewritten as follows

$$\boldsymbol{Z}'_{red} = \boldsymbol{Z}_{pp} - \boldsymbol{Z}_{pw}\boldsymbol{Z}_{ww}^{-1}\boldsymbol{Z}_{wp}, \tag{19}$$

$$\boldsymbol{Y}'_{red} = j\omega[\boldsymbol{P}_{pp} - \boldsymbol{P}_{pw}\boldsymbol{P}_{ww}^{-1}\boldsymbol{P}_{wp}]^{-1}. \tag{20}$$

Based on (19) and (20), the reduced matrices for the resistance $\boldsymbol{R}'$, inductance $\boldsymbol{L}'$ and capacitance $\boldsymbol{C}'$ are expressed as

$$\boldsymbol{R}'_{red} = \boldsymbol{R}_{pp} - \boldsymbol{R}_{pw}\boldsymbol{R}_{ww}^{-1}\boldsymbol{R}_{wp}, \tag{21}$$

$$\boldsymbol{L}'_{red} = \boldsymbol{L}_{pp} - \boldsymbol{L}_{pw}\boldsymbol{L}_{ww}^{-1}\boldsymbol{L}_{wp}, \tag{22}$$

$$\boldsymbol{C}'_{red} = [\boldsymbol{P}_{pp} - \boldsymbol{P}_{pw}\boldsymbol{P}_{ww}^{-1}\boldsymbol{P}_{wp}]^{-1}. \tag{23}$$

In (19)-(23), $\boldsymbol{Z}'_{red}$, $\boldsymbol{Y}'_{red}$, $\boldsymbol{R}'_{red}$, $\boldsymbol{L}'_{red}$ e $\boldsymbol{C}'_{red}$ are the are the longitudinal impedance, transversal admittance, resistance, inductance, and capacitance matrices in their reduced forms, respectively.

## III. Sequence parameters of the transmission line

The sequence voltage $\boldsymbol{V}_{\text{sym}}$ and current $\boldsymbol{I}_{\text{sym}}$ for a multi-circuit transmission line can be expressed as a function the the transformation matrix **S** and its respective voltage $\boldsymbol{V}$ and current $\boldsymbol{I}$ matrices, given by [11]

$$\boldsymbol{V} = \boldsymbol{S}.\boldsymbol{V}_{\text{sym}}, \tag{24}$$

$$\boldsymbol{I} = \boldsymbol{S}.\boldsymbol{I}_{\text{sym}}, \tag{25}$$

where $\boldsymbol{V}_{\text{sym}}$ is the voltage vector and $\boldsymbol{I}_{\text{sym}}$ is the current vector of the symmetrical components. The transformation matrix **S** is given by

$$\boldsymbol{S} = \frac{1}{\sqrt{3}}\begin{bmatrix} 1 & 1 & 1 \\ 1 & \alpha^2 & \alpha \\ 1 & \alpha & \alpha^2 \end{bmatrix}, \tag{26}$$

where $\alpha$ = $e^{j120^\circ}$. Replacing (24) and (25) to (1) and (2), the symmetrical matrices for the impedance ($\boldsymbol{Z'}_{\text{sym}}$) and admittance ($\boldsymbol{Y'}_{\text{sym}}$) for the double-circuit transmission line can be expressed as following [11]

$$\boldsymbol{Z'}_{\text{sym}} = \begin{bmatrix} \boldsymbol{S}^{-1} & 0 \\ 0 & \boldsymbol{S}^{-1} \end{bmatrix} \boldsymbol{Z'}_{\text{red}} \begin{bmatrix} \boldsymbol{S} & 0 \\ 0 & \boldsymbol{S} \end{bmatrix}, \tag{27}$$

$$\boldsymbol{Y'}_{\text{sym}} = \begin{bmatrix} \boldsymbol{S}^{-1} & 0 \\ 0 & \boldsymbol{S}^{-1} \end{bmatrix} \boldsymbol{Y'}_{\text{red}} \begin{bmatrix} \boldsymbol{S} & 0 \\ 0 & \boldsymbol{S} \end{bmatrix}, \tag{28}$$

where the explicit form of $\boldsymbol{Z'}_{\text{sym}}$ and $\boldsymbol{Y'}_{\text{sym}}$ are given by [11]

$$\boldsymbol{Z'}_{\text{sym}} = \begin{bmatrix} \mathrm{Z}^{\mathrm{I}}_{00} & \mathrm{Z}^{\mathrm{I}}_{0+} & \mathrm{Z}^{\mathrm{I}}_{0-} & \mathrm{Z}^{\mathrm{I,II}}_{00} & \mathrm{Z}^{\mathrm{I,II}}_{0+} & \mathrm{Z}^{\mathrm{I,II}}_{0-} \\ \mathrm{Z}^{\mathrm{I}}_{+0} & \mathrm{Z}^{\mathrm{I}}_{++} & \mathrm{Z}^{\mathrm{I}}_{+-} & \mathrm{Z}^{\mathrm{I,II}}_{+0} & \mathrm{Z}^{\mathrm{I,II}}_{++} & \mathrm{Z}^{\mathrm{I,II}}_{+-} \\ \mathrm{Z}^{\mathrm{I}}_{-0} & \mathrm{Z}^{\mathrm{I}}_{-+} & \mathrm{Z}^{\mathrm{I}}_{--} & \mathrm{Z}^{\mathrm{I,II}}_{-0} & \mathrm{Z}^{\mathrm{I,II}}_{-+} & \mathrm{Z}^{\mathrm{I,II}}_{--} \\ \mathrm{Z}^{\mathrm{II,I}}_{00} & \mathrm{Z}^{\mathrm{II,I}}_{0+} & \mathrm{Z}^{\mathrm{II,I}}_{0-} & \mathrm{Z}^{\mathrm{II}}_{00} & \mathrm{Z}^{\mathrm{II}}_{0+} & \mathrm{Z}^{\mathrm{II}}_{0-} \\ \mathrm{Z}^{\mathrm{II,I}}_{+0} & \mathrm{Z}^{\mathrm{II,I}}_{++} & \mathrm{Z}^{\mathrm{II,I}}_{+-} & \mathrm{Z}^{\mathrm{II}}_{+0} & \mathrm{Z}^{\mathrm{II}}_{++} & \mathrm{Z}^{\mathrm{II}}_{+-} \\ \mathrm{Z}^{\mathrm{II,I}}_{-0} & \mathrm{Z}^{\mathrm{II,I}}_{-+} & \mathrm{Z}^{\mathrm{II,I}}_{--} & \mathrm{Z}^{\mathrm{II}}_{-0} & \mathrm{Z}^{\mathrm{II}}_{-+} & \mathrm{Z}^{\mathrm{II}}_{--} \end{bmatrix}, \tag{29}$$

$$\boldsymbol{Y'}_{\text{sym}} = \begin{bmatrix} \mathrm{Y}^{\mathrm{I}}_{00} & \mathrm{Y}^{\mathrm{I}}_{0+} & \mathrm{Y}^{\mathrm{I}}_{0-} & \mathrm{Y}^{\mathrm{I,II}}_{00} & \mathrm{Y}^{\mathrm{I,II}}_{0+} & \mathrm{Y}^{\mathrm{I,II}}_{0-} \\ \mathrm{Y}^{\mathrm{I}}_{+0} & \mathrm{Y}^{\mathrm{I}}_{++} & \mathrm{Y}^{\mathrm{I}}_{+-} & \mathrm{Y}^{\mathrm{I,II}}_{+0} & \mathrm{Y}^{\mathrm{I,II}}_{++} & \mathrm{Y}^{\mathrm{I,II}}_{+-} \\ \mathrm{Y}^{\mathrm{I}}_{-0} & \mathrm{Y}^{\mathrm{I}}_{-+} & \mathrm{Y}^{\mathrm{I}}_{--} & \mathrm{Y}^{\mathrm{I,II}}_{-0} & \mathrm{Y}^{\mathrm{I,II}}_{-+} & \mathrm{Y}^{\mathrm{I,II}}_{--} \\ \mathrm{Y}^{\mathrm{II,I}}_{00} & \mathrm{Y}^{\mathrm{II,I}}_{0+} & \mathrm{Y}^{\mathrm{II,I}}_{0-} & \mathrm{Y}^{\mathrm{II}}_{00} & \mathrm{Y}^{\mathrm{II}}_{0+} & \mathrm{Y}^{\mathrm{II}}_{0-} \\ \mathrm{Y}^{\mathrm{II,I}}_{+0} & \mathrm{Y}^{\mathrm{II,I}}_{++} & \mathrm{Y}^{\mathrm{II,I}}_{+-} & \mathrm{Y}^{\mathrm{II}}_{+0} & \mathrm{Y}^{\mathrm{II}}_{++} & \mathrm{Y}^{\mathrm{II}}_{+-} \\ \mathrm{Y}^{\mathrm{II,I}}_{-0} & \mathrm{Y}^{\mathrm{II,I}}_{-+} & \mathrm{Y}^{\mathrm{II,I}}_{--} & \mathrm{Y}^{\mathrm{II}}_{-0} & \mathrm{Y}^{\mathrm{II}}_{-+} & \mathrm{Y}^{\mathrm{II}}_{--} \end{bmatrix}, \tag{30}$$

where they can be organized as structured matrices given by

$$\boldsymbol{Z'}_{\text{sym}} = \begin{bmatrix} \boldsymbol{Z}^{\mathrm{I}} & \boldsymbol{Z}^{\mathrm{I,II}} \\ \boldsymbol{Z}^{\mathrm{II,I}} & \boldsymbol{Z}^{\mathrm{II}} \end{bmatrix}, \tag{31}$$

$$\boldsymbol{Y'}_{\text{sym}} = \begin{bmatrix} \boldsymbol{Y}^{\mathrm{I}} & \boldsymbol{Y}^{\mathrm{I,II}} \\ \boldsymbol{Y}^{\mathrm{II,I}} & \boldsymbol{Y}^{\mathrm{II}} \end{bmatrix}. \tag{32}$$

Based on (31), the sequence impedance matrix $\boldsymbol{Z'}_{\text{sym}}$ of a double-circuit transmission line can be organized as a set of sub-matrices: The $\boldsymbol{Z}^{\mathrm{I}}$ and $\boldsymbol{Z}^{\mathrm{II}}$ represents the magnetic and electric couplings internally related to their own circuit (I or II), being formed by self elements in the main diagonal, $Z^{\mathrm{c}}_{\mathrm{jj}}$, and by the mutual elements off the main diagonal $Z^{\mathrm{c}}_{\mathrm{ij}}$ for (i,j) $\in \{0, +, -\}$ and c $\in \{\mathrm{I}, \mathrm{II}\}$. Furthermore, the sub-matrices $\boldsymbol{Z}^{\mathrm{I,II}}$ and $\boldsymbol{Z}^{\mathrm{II,I}}$ are related to the magnetic and electric couplings between the circuits I and II, represented by self elements in the main diagonal $Z^{\mathrm{I,II}}_{\mathrm{ii}}$ and by mutual elements in off main diagonal $Z^{\mathrm{I,II}}_{\mathrm{ij}}$. The same pattern is obtained for the sequence admittance matrix $\boldsymbol{Y'}_{\text{sym}}$ in (32).

A generic representation of these sequence circuits is illustrated in Fig. 2, showing some of the mutual couplings. According to this figure, each sequence circuit (I, II) has its own internal coupling (dashed lines) and external coupling between both circuits (solid lines). It is worth mentioning that for ideally transposed double-circuit transmission lines, the sequence matrices ($\boldsymbol{Z'}_{\text{sym}}$) and ($\boldsymbol{Y'}_{\text{sym}}$) have only non-zero elements on the main diagonal ($Z^{\mathrm{c}}_{\mathrm{jj}} \neq 0$ and $Y^{\mathrm{c}}_{\mathrm{jj}} \neq 0$), for j $\in \{0, +, -\}$ and c $\in \{\mathrm{I}, \mathrm{II}\}$. The transmission line parameters can be explicitly expressed as follows

$$\mathrm{Z}'_{\mathrm{ii}} = \mathrm{R}'_{\mathrm{ii}} + j\omega \mathrm{L}'_{\mathrm{ii}}, \tag{33}$$

$$\mathrm{Z}'_{\mathrm{ik}} = \mathrm{R}'_{\mathrm{ik}} + j\omega \mathrm{L}'_{\mathrm{ik}}, \tag{34}$$

$$\mathrm{Y}'_{\mathrm{ii}} = \mathrm{G}'_{\mathrm{ii}} + j\omega \mathrm{C}'_{\mathrm{ii}}, \tag{35}$$

$$\mathrm{Y}'_{\mathrm{ik}} = \mathrm{G}'_{\mathrm{ik}} + j\omega \mathrm{C}'_{\mathrm{ik}}. \tag{36}$$

The self transmission line parameters- resistance ($\mathrm{R}'_{\mathrm{ii}}$), inductance ($\mathrm{L}'_{\mathrm{ii}}$) and capacitance ($\mathrm{C}'_{\mathrm{ii}}$) will be investigated in the further section. The conductance ($\mathrm{G}'_{\mathrm{ii}}$) is neglected. Additionally, the influence of the mutual elements are also investigated as a function of the frequency.

## IV. Numerical results

In order to investigate the influence of the frequency-dependent soil electrical parameters on the sequence parameters, three distinct transmission lines are considered, as illustrated in Fig. 3, being denoted as Danube, Flat and Ton, as detailed in [8]. For this purpose, the ground-return impedance and admittance are calculated using the Nakagawa's approach, using equations from (5) to (12) considering a soil with low-frequency resistivity $\rho_0$ of 1,000 Ω.m using the expressions in (13) and (14). The per-unit-length (pul) resistance, inductance and capacitance, as well as the coupling factors between the one and both circuits are calculated in the frequency range of 100 Hz to 1 MHz. The electrical DC resistance $R_{\mathrm{DC}}$ and radius of the phase conductors ($r_{\mathrm{C}}$) and ground wires (GW) ($r_{\mathrm{GW}}$) are indicated in the Fig. 3. The simulations were conducted using a custom MATLAB program [18]. The numerical results are divided into the following sections:

### A. Series Resistance and Inductance of Sequence parameters

The calculated pul resistance and inductance for the positive and zero sequences of the investigated transmission tower are shown in Figs. 4 and 5, respectively. According to Fig. 4-(b), the zero resistance is significantly higher than the positive resistance illustrated in Fig. 4-(a) across the analyzed frequency range. Additionally, the sequence resistance obtained for tower Ton (shown in green lines) differs considerably from the other two towers. The higher value of the zero resistance arises from the identical phase angles of the zero sequence currents flowing in the double-circuit transmission line. Consequently, residual currents flow through both the earth and the ground

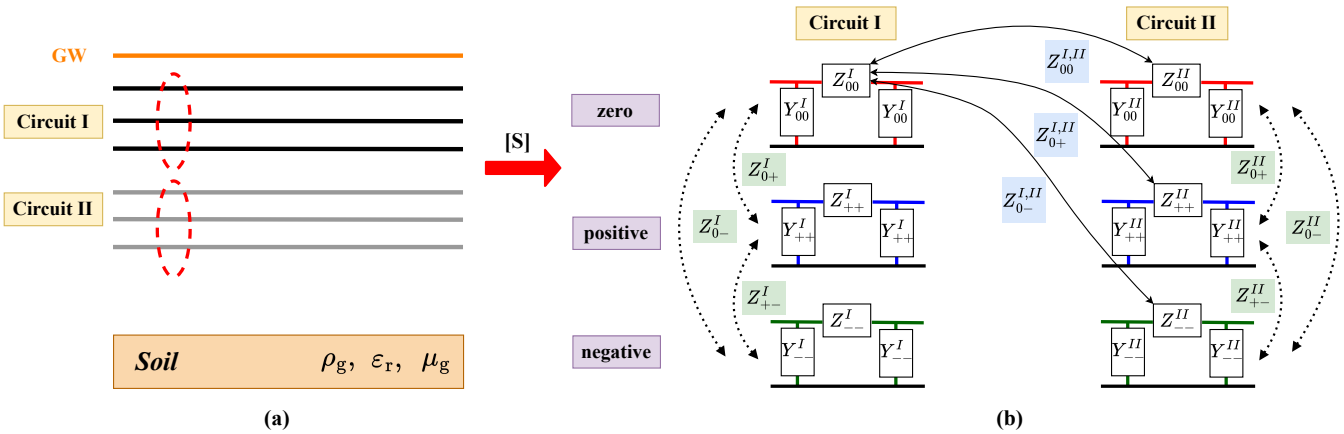


Fig. 2: (a) Double-circuit transmission line with one ground wire (GW) located on a generic soil; (b) Zero (in red), positive (in blue) and negative (in green) sequence circuits with some of their internal coupling inside each circuit (dashed lines) and external coupling between circuits (solid lines).

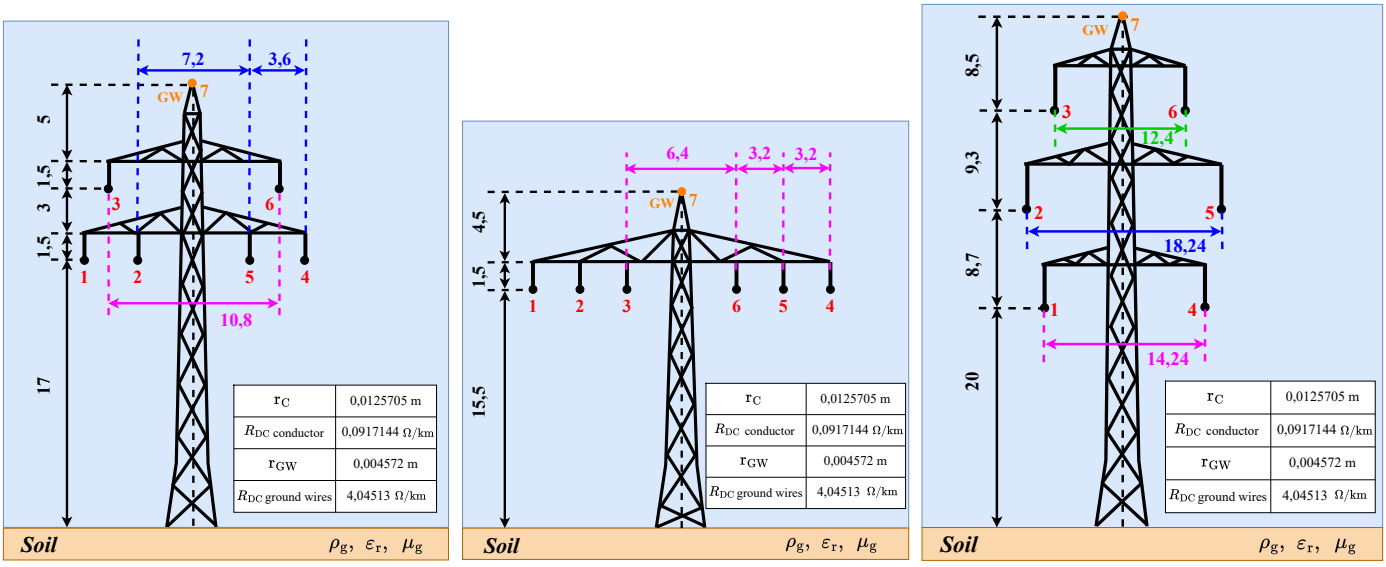


Fig. 3: Tower configurations used in this study: (a) Danube; (b) Flat and (c) Ton. (all measures in meters, not to scale)

wires [8]. Thus, this zero resistance accounts for the configuration formed by the ground wires, transmission line resistance, and earth-return impedance. Given that earth-return impedance increases with frequency, the zero resistance is expected to rise accordingly. Conversely, the positive resistance is smaller because no loop forms in the circuit line. It is noteworthy that the negative and positive resistances are identical.

Concerning the sequence inductance plotted in Fig. 5, it can be observed that the positive inductance shown in Fig. 5-(a) is smaller than the zero inductance depicted in Fig. 5-(b) across the frequency range. The positive inductance exhibits minimal variation with frequency because no loops are formed between the ground wires and earth in the positive sequence. In contrast, the zero inductance shows a more pronounced variation, decreasing gradually as the frequency increases. This behavior is attributed to the penetration depth of the return currents flowing in the soil for the zero sequence, which decreases with increasing frequency [8]. The Ton tower exhibits the most divergent behavior compared to the other towers, owing to its greater height and the larger distances between the phase conductors.

### *B. Shunt Capacitance of the Sequence parameters*

The sequence capacitance is plotted in Fig. 6. According to this figure, the positive capacitance remains constant with frequency, as depicted in Fig. 6-(a). This behavior is related to the external capacitance, which is not affected by either the frequency or the soil's electrical parameters, depending only on the geometrical parameters of the transmission line. Furthermore, the positive capacitance is much higher than the

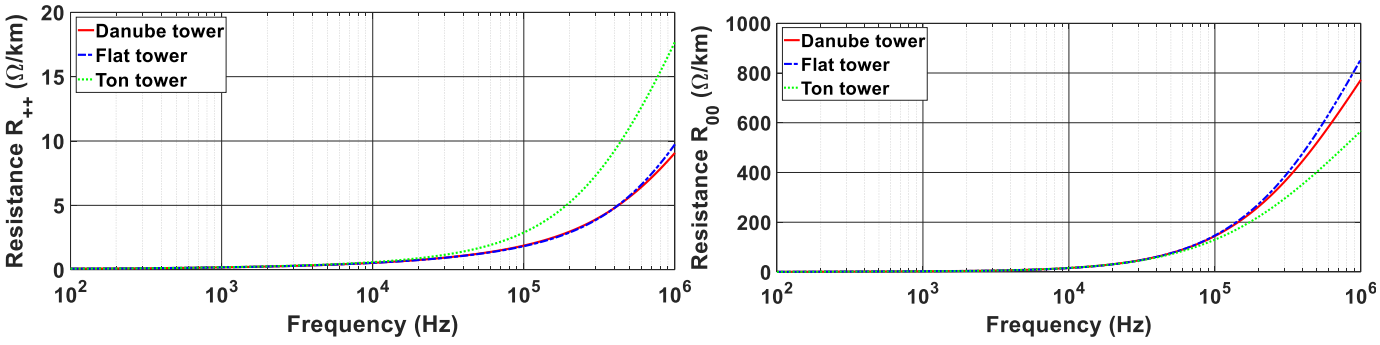


(a) (b)

Fig. 4: Calculated pul resistance assuming FD soil of $\rho_0$ = 1,000 Ω.m: (a) positive $R_{++}$; (b) zero $R_{00}$.

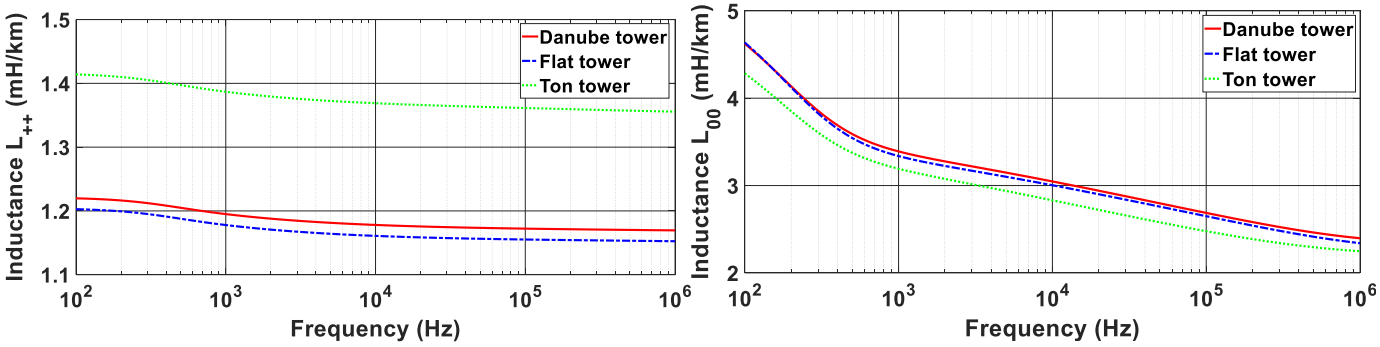


(a) (b)

Fig. 5: Calculated pul inductance assuming FD soil of $\rho_0$ = 1,000 Ω.m: (a) positive $L_{++}$; (b) zero $L_{00}$.

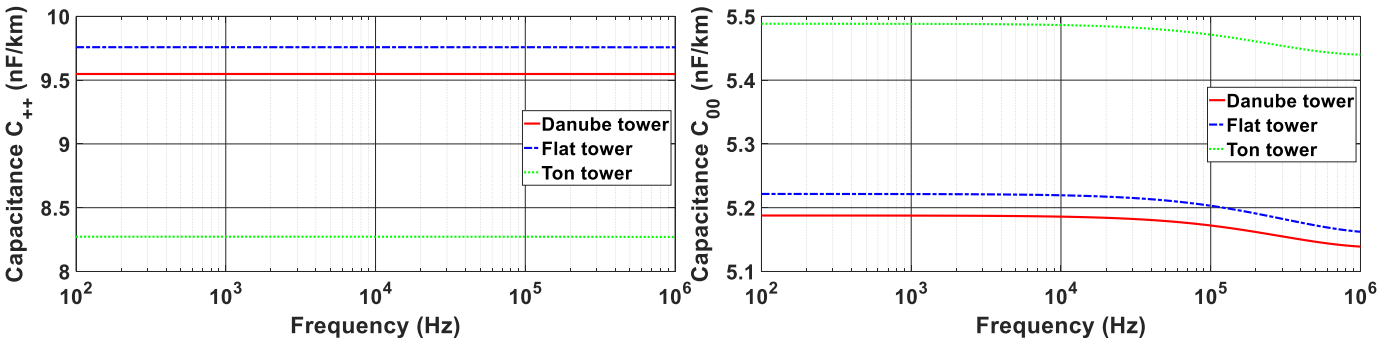


(a) (b)

Fig. 6: Calculated pul capacitance assuming FD soil of $\rho_0$ = 1,000 Ω.m: (a) positive $C_{++}$; (b) zero $C_{00}$.

zero capacitance, as illustrated in Fig. 6-(b). However, the zero capacitance gradually decreases as the frequency increases due to the ground-return admittance $\boldsymbol{Y}_{\mathrm{g}}$ added to the transversal admittance $\boldsymbol{Y}_{\mathrm{t}}$ in (4). This behavior is expected since the total capacitance decreases at higher frequencies when the frequency dependence of the soil is taken into account in the ground-return admittance, as detailed in [19] [see Figs. 21, 22, and 26]. Finally, the Ton tower has exhibited the most divergent values due its higher distances between the phase conductors compared to the other tower configurations.

### *C. Mutual impedance and Admittance between the Sequences of one circuit*

In the context of double-circuit transmission line topologies, the untransposed configuration leads to coupling impedances and admittances that must be considered for accurate sequence circuit representation. These couplings exist due to the unequal distances between phase conductors, ground wires and earth [8]. Additionally, the unequal distance between the two circuits result in coupling between the impedances and admittances in the sequence circuits, as illustrated in Fig. 2. These coupling

effects are crucial for the precise computation of fault locations, power flow analysis, and power quality assessments. In order to assess the impact of the coupling withing one circuit, the following normalized coupling factors are defined

$$\Delta_1 = \left|\frac{\mathrm{Z}^{\mathrm{I}}_{0+}}{\mathrm{Z}^{\mathrm{I}}_{00}}\right|, \Delta_2 = \left|\frac{\mathrm{Z}^{\mathrm{I}}_{0-}}{\mathrm{Z}^{\mathrm{I}}_{00}}\right|, \Delta_3 = \left|\frac{\mathrm{Z}^{\mathrm{I}}_{+-}}{\mathrm{Z}^{\mathrm{I}}_{00}}\right|, \Delta_4 = \left|\frac{\mathrm{Z}^{\mathrm{I}}_{-+}}{\mathrm{Z}^{\mathrm{I}}_{00}}\right|, \tag{37}$$

$$\Delta_5 = \left|\frac{\mathrm{Y}^{\mathrm{I}}_{0+}}{\mathrm{Y}^{\mathrm{I}}_{00}}\right|, \Delta_6 = \left|\frac{\mathrm{Y}^{\mathrm{I}}_{0-}}{\mathrm{Y}^{\mathrm{I}}_{00}}\right|, \Delta_7 = \left|\frac{\mathrm{Y}^{\mathrm{I}}_{+-}}{\mathrm{Y}^{\mathrm{I}}_{00}}\right|, \Delta_8 = \left|\frac{\mathrm{Y}^{\mathrm{I}}_{-+}}{\mathrm{Y}^{\mathrm{I}}_{00}}\right|, \tag{38}$$

where coupling factors from $\Delta_1$ to $\Delta_4$ assess the coupling impedance based on the self zero impedance $Z^{\mathrm{I}}_{00}$ and those from $\Delta_5$ to $\Delta_8$ assess the coupling admittance based on the self zero admittance $Y^{\mathrm{I}}_{00}$. The calculated coupling factors $\Delta_1$ to $\Delta_8$ for each tower topology are plotted in Fig. 7.

According to this figure, the results demonstrate that the coupling factors $\Delta_1$, $\Delta_2$, $\Delta_3$, and $\Delta_4$ do not exceed 4% for zero impedance, indicating a slight dependence on the frequency of the mutual magnetic coupling in the sequence circuit. On the other hand, the coupling factors $\Delta_5$, $\Delta_6$, $\Delta_7$, and $\Delta_8$ for zero admittance remain constant across the entire frequency range. However, higher magnitudes are observed, suggesting that the electric coupling in the sequence admittances cannot be disregarded. Additionally, these coupling factors are also dependent on the tower topology due to their distances between the phase conductors and distance from earth to the conductors.

### *D. Mutual impedance and Admittance between the Sequences of both circuits*

To investigate the effect of the electric and magnetic coupling on the two sequence circuits of the double-circuit transmission lines, the coupling factors (CF) between both circuit are defined as follows

$$\delta_1 = \left|\frac{\mathrm{Z}^{\mathrm{I,II}}_{00}}{\mathrm{Z}^{\mathrm{I}}_{00}}\right|, \quad \delta_2 = \left|\frac{\mathrm{Z}^{\mathrm{I,II}}_{++}}{\mathrm{Z}^{\mathrm{I}}_{00}}\right|, \tag{39}$$

$$\delta_3 = \left|\frac{\mathrm{Y}^{\mathrm{I,II}}_{00}}{\mathrm{Y}^{\mathrm{I}}_{00}}\right|, \quad \delta_4 = \left|\frac{\mathrm{Y}^{\mathrm{I,II}}_{++}}{\mathrm{Y}^{\mathrm{I}}_{00}}\right|. \tag{40}$$

The coupling factors $\delta_1$ and $\delta_2$ calculate the magnetic coupling based on the self zero impedance $Z^{\mathrm{I}}_{00}$, whereas $\delta_3$ and $\delta_4$ compute the electric coupling based on the self zero admittance $Y^{\mathrm{I}}_{00}$. The coupling factors (CF) $\delta_1$, $\delta_2$, $\delta_3$, and $\delta_4$ for each tower topology are plotted in Fig. 8.

According to this figure, it is noted that $\delta_1$ exhibits high CF values for both electric and magnetic coupling between sequence circuits. Results demonstrate that the CF is approximately 60% at low frequencies and decreases gradually with increasing frequency until it reaches 30%, indicating a stronger relation between the two sequence circuits. However, the coupling factor $\delta_2$ remains very small across the entire frequency range. Regarding the coupling factors $\delta_3$ and $\delta_4$ for the self zero admittance, it is observed that $\delta_3$ ranges between 20% and 30% at lower frequencies, depending on the tower topology. Furthermore, the CF $\delta_3$ increases slightly with increasing frequency but still represents a considerable value. On the other hand, the CF $\delta_4$ remains constant across the frequency range, not exceeding 5%. These results demonstrate that the magnetic and electric coupling related to the zero sequence between both circuits is stronger than that observed for the positive sequence. As an alternative to reduce the coupling effects between both sequence circuits, a transposition configuration can be applied to the double-circuit transmission line, resulting in decoupled sequence matrices [11], [12].

## V. Conclusions

This paper investigated the sequence parameters of three distinct double-circuit transmission lines (Danube, Flat, and Ton), assuming an untransposed configuration, ground-return effect on the longitudinal impedance and transversal admittance matrices modeled by Nakagawa's approach. Additionally, the frequency dependence of the soil electrical parameters was taken into account, with a low-frequency soil resistivity of 1,000 Ω.m for a frequency range from 100 Hz to 1 MHz.

Firstly, the per-unit-length transmission line parameters (resistance, inductance, and capacitance) for both zero and positive sequences were calculated over that frequency range. The results indicated that the zero-sequence resistance and inductance are considerably higher than those for the positive sequence across the frequency range. This occurs due to the zero-sequence currents (same magnitude and phase) flowing through the earth path and ground wire. Furthermore, the sequence parameters are also significantly dependent on the tower topology (height and distances of the phase conductors). The positive-sequence capacitance is higher in magnitude but is not affected by frequency. However, the zero-sequence capacitance varies at high frequencies due to the ground-return admittance.

Finally, the coupling factors for one circuit and between both circuits were calculated for the double-circuit transmission lines. It is shown that the coupling factor within one circuit, when normalized to the zero-sequence impedance, can be neglected. However, the coupling factor for the zero-sequence admittance can be considerable depending on the tower topology. Regarding the coupling factor between the two circuits, results indicated that the magnitude of the zero-sequence impedance is significant across the frequency range. These results confirm that the magnetic and electric coupling between both circuits in the zero sequence is strong for untransposed double-circuit overhead transmission lines. As a contribution, this demonstrated that for untransposed double-circuit transmission lines, the electric and magnetic coupling between both circuits cannot be neglected when building the sequence circuits, especially if high frequency events are involved in the simulations.

## References

[1] S. Das, S. Santoso, R. Horton, and A. Gaikwad, "Effect of earth current return model on transmission line fault location - a case study," in *2013 IEEE Power & Energy Society General Meeting*, 2013, pp. 1–5.

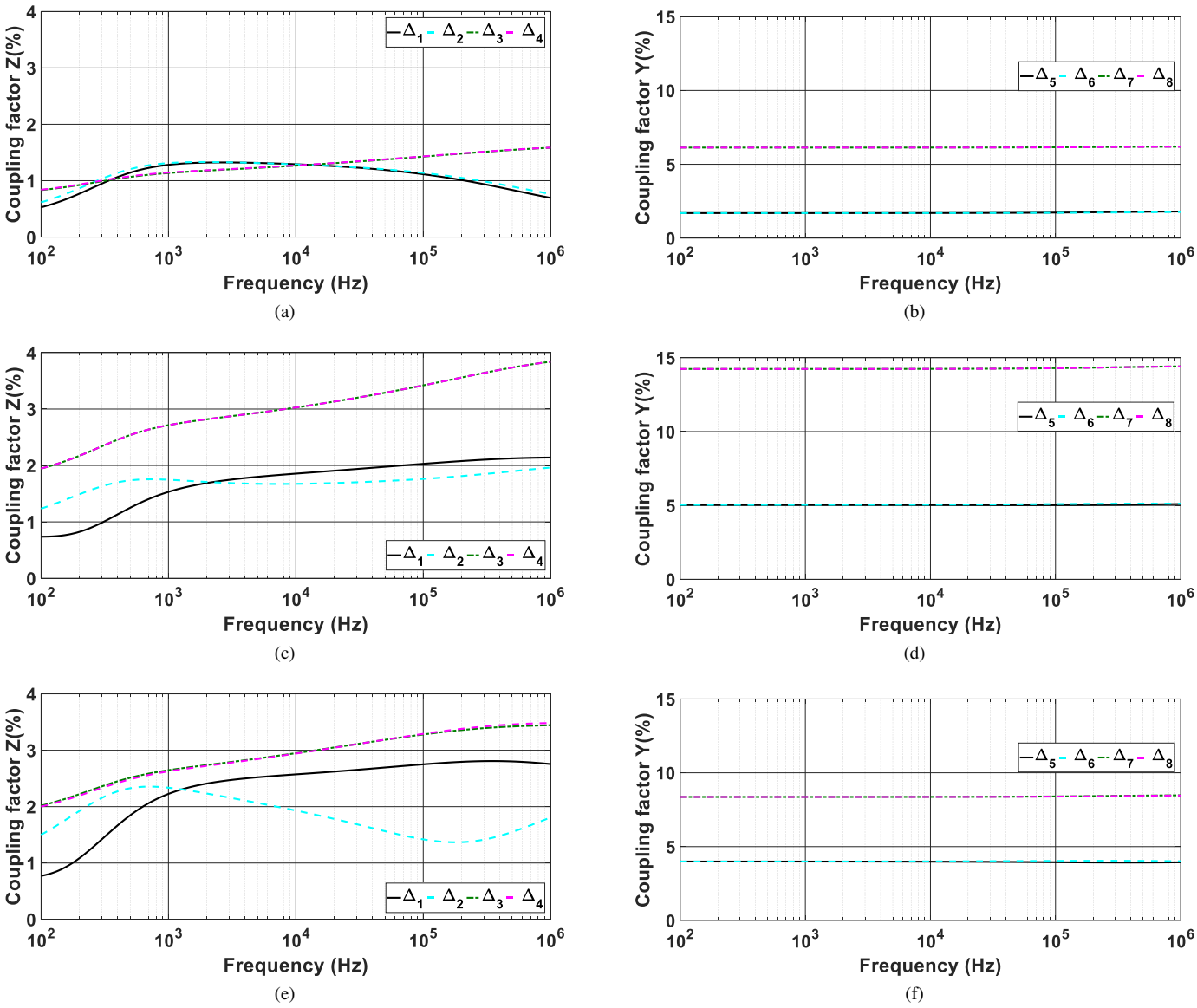


Fig. 7: Coupling factors related to one circuit for the zero sequence impedance [on the left side] and zero sequence admittance [on the right side] for the towers: (a) - (b) Danube; (c) - (d) Flat and (e) - (f) Ton.

[2] W. Xiu and Y. Liao, "Online one-end fault location algorithm for parallel transmission lines," *Smart Grid and Renewable Energy*, vol. 2, no. 4, pp. 359–366, 2011.

[3] A. Dziendziel, H. Kocot, and P. Kubek, "Construction and modeling of multi-circuit multi-voltage hvac transmission lines," *Energies*, vol. 14, no. 2, 2021. [Online]. Available: https://www.mdpi.com/1996-1073/14/2/421

[4] S. Das, S. N. Ananthan, and S. Santoso, "Estimating zero-sequence impedance of three-terminal transmission line and thevenin impedance using relay measurement data," *Protection and Control of Modern Power Systems*, vol. 3, no. 4, pp. 1–10, 2018.

[5] M. Gil, A. A. Abdoos, and M. Sanaye-Pasand, "A precise analytical method for fault location in double-circuit transmission lines," *International Journal of Electrical Power & Energy Systems*, vol. 126, p. 106568, 2021.

[6] Z. Xu, "Live line measuring the parameters of 220 kv transmission lines with mutual inductance in hainan power grid," *Engineering*, vol. 05, pp. 146–151, 01 2013.

[7] H. Goklani, G. Gajjar, and S. A. Soman, "Quantification of minimum unbalance required for accurate estimation of sequence parameters of transmission line using pmu data," in *2019 IEEE Power & Energy Society General Meeting (PESGM)*, 2019, pp. 1–5.

[8] L. Pop, K. Malekian, A. Hoshmeh, and W. Schufft, "Investigation of frequency-dependent impedance and admittance of 110-kv overhead lines using symmetrical components," in *2017 11th IEEE International Conference on Compatibility, Power Electronics and Power Engineering (CPE-POWERENG)*. IEEE, 2017, pp. 59–64.

[9] J. R. Carson, "Wave propagation in overhead wires with ground return," *The Bell System Technical Journal*, vol. 5, no. 4, pp. 539–554, 1926.

[10] M. Nakagawa, "Admittance correction effects of a single overhead line," *IEEE Transactions on Power Apparatus and Systems*, no. 3, pp. 1154–1161, 1981.

[11] N. D. Tleis, "3 - Modelling of multi-conductor overhead lines and cables," in *Power Systems Modelling and Fault Analysis*, ser. Newnes Power Engineering Series, N. D. Tleis, Ed. Oxford: Newnes, 2008, pp. 74–199.

[12] G. Radhika, "Computation of 400 kV Phase and Sequence Impedance Matrices Signifying Transposition," *i-Manager's Journal on Power*

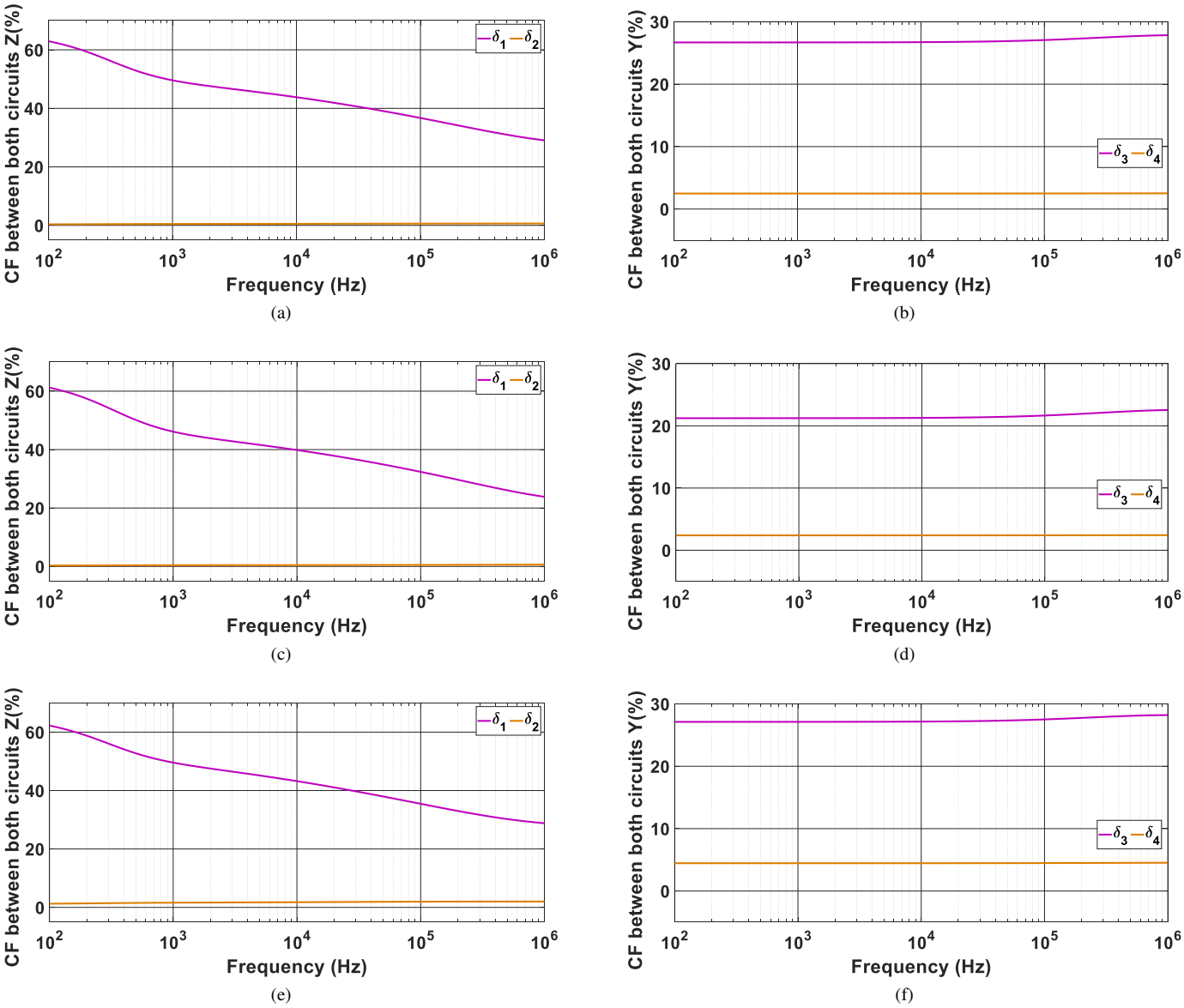


Fig. 8: Coupling factors between to both circuits for the zero sequence impedance [on the left side] and zero sequence admittance [on the right side] for the towers: (a) - (b) Danube; (c) - (d) Flat and (e) - (f) Ton.

*Systems Engineering*, vol. 3, no. 3, p. 1, 2015.

[13] A. Piantini, *Lightning Interaction with Power Systems: Applications, Volume 2*, ser. Energy Engineering. Institution of Engineering and Technology, 2020. [Online]. Available: https://books.google.com.br/books?id=pFvUDwAAQBAJ

[14] W. G. CIGRE C4.33, "Impact of soil-parameter frequency dependence on the response of grounding electrodes and on the lightning performance of electrical systems," *Tech. Brochure 781*, pp. 1–66, 2019.

[15] S. Kurokawa, J. Filho, M. Tavares, C. Portela, and A. Prado, "Behavior of overhead transmission line parameters on the presence of ground wires," *IEEE Transactions on Power Delivery*, vol. 20, no. 2, pp. 1669–1676, 2005.

[16] A. P. Moura, A. A. F. Moura, and E. P. Rocha, *Transmissão de energia elétrica em corrente alternada*. Fortaleza, Brasil: Editora da Universidade Federal do Ceará, 2019.

[17] P. Torrez Caballero, "Inclusion of the frequency dependence in the bergeron model: representation of short and long transmission lines considering electromagnetic transients resulting from switching operations and lightning strikes," *Thesis (PhD in electrical engineering)*, 2018.

[18] T. M. Inc., "Matlab version: 9.13.0 (r2022b)," Natick, Massachusetts, United States, 2022. [Online]. Available: https://www.mathworks.com

[19] J. Gertrudes, M. Tavares, and C. Portela, "Influência da dependência de parâmetros do solo com a frequência na modelagem de linhas aéreas de transmissão: caso de condutor único," *Sba: Controle & Automação Sociedade Brasileira de Automatica*, vol. 22, pp. 506–522, 2011.